



A NEW APPROACH TO ARRAY INTERPOLATION BY GENERATION OF ARTIFICIAL SHIFT INVARIANCES: INTERPOLATED ESPRIT

Markus Bühren

Marius Pesavento

Johann F. Böhme

Chair of System Theory and Signal Processing
Universität Stuttgart, D-70569 Stuttgart, Germany
markus.buehren@lss.uni-stuttgart.de

Dept. of Electrical Engineering and Information Sciences
Ruhr-Universität Bochum, D-44780 Bochum, Germany
{mps, boehme}@sth.ruhr-uni-bochum.de

ABSTRACT

We address the problem of data independent robust array interpolation over large angular sectors. Previous interpolation methods apply the root-MUSIC principle to interpolation data of a predefined virtual ULA manifold. These methods either suffer from severely biased direction-of-arrival estimates due to interpolation errors or rely on data dependent interpolation matrix design. In this paper a new interpolation approach is proposed. Instead of transforming the original array geometry to the rather restrictive ULA structure, here interpolation is performed with the objective to create a virtual array manifold which is a shifted version of the real array manifold. This artificial shift-invariance can be exploited by the well-known ESPRIT algorithm. A joint design of virtual array geometry and interpolation matrix yields additional degrees of freedom which reduce interpolation errors and allow to increase the interpolation sector. The new algorithm enjoys both simple design procedure and fast implementation and offers reliable DOA estimation for a wide range of different scenarios.

1. INTRODUCTION

Specific redundancies in array structures can be exploited to simplify implementations of subspace direction finding methods. For example, the Uniform Linear Array (ULA) allows the formulation of the computationally efficient search-free root-MUSIC and MODE algorithms [1], [2]. Similarly, sensor arrays with shift-invariances facilitate search-free formulations of subspace methods, as for example conventional and multiple invariance ESPRIT [3], UCA root-MUSIC and UCA-ESPRIT [4], multiple invariance root-MUSIC [5] and RARE [6].

The idea of array interpolation techniques is to make search-free estimation methods applicable to the general class of “non-structured” arrays. An early approach by Friedlander [7] is based on a linear transformation of the original array manifold to a desired ULA manifold over a preliminary defined directional sector. Even though this

method has several attractive properties, it is bounded to comparably small interpolation sectors and its DOA estimation performance is severely limited by a strong bias in the root-MUSIC estimates. The bias results from interpolation errors between the interpolated and the desired array response. Several authors have addressed this issue and numerous methods have been designed to essentially reduce the bias [8], [9]. Unfortunately, these methods incorporate data measurements into the interpolation matrix design and therefore require the matrix computation to be done “on-line”, leading to increased computational complexity.

In this paper, we propose a new interpolation method which is based on the idea of including the virtual array design into the interpolation matrix design procedure. Instead of performing an interpolation onto a preliminary specified array structure, in the new approach the virtual array is designed to be a mathematically shifted version of the original array. In contrast to [10], the virtual array manifold is not limited to belong to a physically realizable array structure. Note that this artificially generated shift-invariance does not make any demands on the physical array structure like conventional ESPRIT does.

Relaxation of the restrictions imposed on the virtual array yields several important advantages: reduction of interpolation error and estimation bias which allows to increase the extent of the sector that interpolation can successfully be applied on, simplification of the interpolation design and reliability of the solution in many different scenarios.

2. ARRAY SIGNAL MODEL

Consider a sensor array composed of N sensor elements with the n th sensor located at the position $d_{x,n}$ and $d_{y,n}$ in the x - and y -direction, respectively. Let L narrowband plane waves impinge on the array from unknown DOAs. For simplicity, we assume that all signal sources are located in the x - y -plane where the DOA of the l th source signal is fully represented by its azimuth angle $\theta_l \in [0, 2\pi]$ measured counterclockwise from the x -axis. The array response to a source signal arriving from the DOA θ is given by $\mathbf{a}(\theta) =$

$[e^{-jk(d_{x,1}\cos\theta+d_{y,1}\sin\theta)}, \dots, e^{-jk(d_{x,N}\cos\theta+d_{y,N}\sin\theta)}]^T$
where $(\cdot)^T$ denotes transposition and k denotes the wave-number. The array output vector can be modeled as

$$\mathbf{x}(t) = \mathbf{A}(\boldsymbol{\theta}) \mathbf{s}(t) + \mathbf{n}(t), \quad t = 1, 2, \dots, M \quad (1)$$

where

$$\mathbf{A}(\boldsymbol{\theta}) = [\mathbf{a}(\theta_1), \dots, \mathbf{a}(\theta_L)] \quad (2)$$

is the $(N \times L)$ steering matrix, $\boldsymbol{\theta} = [\theta_1, \dots, \theta_L]^T$ is the vector of true source DOAs, $\mathbf{s}(t)$ is the $(L \times 1)$ vector containing the complex signal envelopes, $\mathbf{n}(t)$ is the $(N \times 1)$ vector of zero-mean spatially white sensor noise of variance σ_n^2 and M is the number of snapshots. The spatial covariance matrix corresponding to (1) and its eigendecomposition are given by

$$\begin{aligned} \mathbf{R} &= \mathbb{E}\{\mathbf{x}(t)\mathbf{x}^H(t)\} = \mathbf{A}(\boldsymbol{\theta}) \mathbf{S} \mathbf{A}^H(\boldsymbol{\theta}) + \sigma_n^2 \mathbf{I} \\ &= \mathbf{E}_s \mathbf{\Lambda}_s \mathbf{E}_s^H + \mathbf{E}_n \mathbf{\Lambda}_n \mathbf{E}_n^H \end{aligned} \quad (3)$$

where $\mathbf{S} = \mathbb{E}\{\mathbf{s}(t)\mathbf{s}^H(t)\}$ is the $(L \times L)$ source covariance matrix, \mathbf{I} is the identity matrix, $(\cdot)^H$ denotes Hermitian transposition and $\mathbb{E}\{\cdot\}$ is the statistical expectation operator. The $(L \times L)$ and the $(N-L) \times (N-L)$ diagonal matrices $\mathbf{\Lambda}_s$ and $\mathbf{\Lambda}_n$ contain the signal- and noise-subspace eigenvalues of \mathbf{R} , respectively. In turn, the columns of the $(N \times L)$ and $N \times (N-L)$ matrices \mathbf{E}_s and \mathbf{E}_n denote the corresponding signal- and noise-subspace eigenvectors. Similarly, the sample estimate of the covariance matrix (3) can be decomposed as

$$\hat{\mathbf{R}} = \frac{1}{M} \sum_{t=1}^M \mathbf{x}(t)\mathbf{x}^H(t) = \hat{\mathbf{E}}_s \hat{\mathbf{\Lambda}}_s \hat{\mathbf{E}}_s^H + \hat{\mathbf{E}}_n \hat{\mathbf{\Lambda}}_n \hat{\mathbf{E}}_n^H. \quad (4)$$

3. VIRTUAL SHIFT INVARIANCES

The idea of conventional array interpolation techniques is a transformation of the real array manifold over a given angular sector $\Theta = [\theta_{\min}, \theta_{\max}]$ onto a preliminary specified virtual array manifold. That is, a $(\check{N} \times N)$ interpolation matrix \mathbf{B} is designed that satisfies

$$\mathbf{B}\mathbf{a}(\boldsymbol{\theta}) \approx \check{\mathbf{a}}(\boldsymbol{\theta}), \quad \boldsymbol{\theta} \in \Theta \quad (5)$$

where $\mathbf{a}(\boldsymbol{\theta})$ and $\check{\mathbf{a}}(\boldsymbol{\theta})$ are the $(N \times 1)$ and $(\check{N} \times 1)$ steering vectors of the real and virtual array, respectively, and \check{N} is the number of virtual sensors. The virtual array manifold $\check{\mathbf{a}}(\boldsymbol{\theta})$ usually corresponds to a uniform linear array (ULA). A major difficulty emerging in this approach is the comparably restrictive constraint imposed by the a priori choice of the virtual array geometry.

Moreover, conventional array interpolation techniques share the fact that the selection of the parameters that define the virtual ULA geometry and allow best interpolation and estimation results is not a part of the optimization problem

which is formulated for the interpolation matrix calculation. The parameters in question are the number of virtual sensors, the inter-element spacing, the array orientation and the position of the array center and are chosen heuristically.

In this paper we present a new interpolation approach which has the ability to overcome those drawbacks. Instead of an interpolation from the real array manifold to a predefined ULA manifold, here the target geometry is a shifted version of the real array manifold:

$$\check{\mathbf{a}}(\boldsymbol{\theta}) = z(\boldsymbol{\theta}) \mathbf{a}(\boldsymbol{\theta}), \quad \boldsymbol{\theta} \in \Theta. \quad (6)$$

The phase shift $z(\boldsymbol{\theta}) \in \mathbb{C}$ may theoretically be any invertible function; we recommend to use an exponential form like $z(\boldsymbol{\theta}) = e^{j\theta}, e^{j2\pi\cos(\theta)}$ or $e^{j2\pi\sin(\theta)}$. Note that due to the construction of the virtual array we have $\check{N} = N$ here.

The computation of the interpolation matrix \mathbf{B} is now done in accordance to Friedlander's method [7]. K representative directions $\theta_1, \dots, \theta_K$ are chosen from the interpolation sector Θ . The sum of the quadratic interpolation errors in these directions,

$$F(\mathbf{B}) = \sum_{i=1}^K \| \mathbf{B} \mathbf{a}(\theta_i) - \check{\mathbf{a}}(\theta_i) \|^2 = \| \mathbf{B} \mathbf{C} - \check{\mathbf{C}} \|^2_F, \quad (7)$$

is minimized with respect to \mathbf{B} . In the last equality we used the matrix \mathbf{C} consisting of the steering vectors of the sample directions: $\mathbf{C} = [\mathbf{a}(\theta_1), \dots, \mathbf{a}(\theta_K)]$. Similarly, $\check{\mathbf{C}}$ contains the virtual steering vectors and is calculated as $\check{\mathbf{C}} = \mathbf{C} \mathbf{Z}$, where \mathbf{Z} contains the shifting terms:

$$\mathbf{Z} = \text{diag}\{z(\theta_1), \dots, z(\theta_K)\} \quad (8)$$

The minimizing argument of the least-squares optimization criterion (7) can now easily be calculated as $\mathbf{B} = \check{\mathbf{C}}\mathbf{C}^\dagger$, where $(\cdot)^\dagger$ denotes the Moore-Penrose pseudoinverse of an arbitrary matrix; $\mathbf{C}^\dagger = (\mathbf{C}^H \mathbf{C})^{-1} \mathbf{C}^H$ in the case that the involved inverse is defined. Note that this calculation of high computational effort has to be done only in the design phase, not in the "online" algorithm application.

Even if we are only generating a shifted version of the array manifold, the noise characteristics of the original and transformed output signals can be quite different. The covariance matrix of the real array is defined in (3), whereas the covariance matrix of the virtual array is given by

$$\check{\mathbf{R}} = \mathbf{B} \mathbf{R} \mathbf{B}^H = \check{\mathbf{A}} \check{\mathbf{S}} \check{\mathbf{A}}^H + \sigma_n^2 \mathbf{B} \mathbf{B}^H, \quad (9)$$

with $\check{\mathbf{A}} = \mathbf{B} \mathbf{A}(\boldsymbol{\theta})$. Obviously, the sensor noise of the virtual array is generally colored. In [7], where the root-MUSIC algorithm is applied to a virtual uniform linear array, noise-prewhitening by multiplication with $(\mathbf{B} \mathbf{B}^H)^{-1/2}$ is inevitable. In practice the prewhitening matrix is often ill-conditioned, leading to numerical difficulties in the estimation procedure. Here, where we use the ESPRIT

algorithm instead, noise-prewhitening would destroy the shift-invariance relating the physical to the virtual array. A more sophisticated procedure, which turns out to yield essential benefits, is developed from the singular-value-decomposition of the interpolation matrix

$$\mathbf{B} = \mathbf{U} \boldsymbol{\Gamma} \mathbf{V}^H \quad (10)$$

with the unitary ($N \times N$) matrices \mathbf{U} and \mathbf{V} and the ($N \times N$) diagonal matrix $\boldsymbol{\Gamma}$ containing the singular values of \mathbf{B} arranged in non-increasing order. Multiplying both sides of equation (5) with \mathbf{U}^H from the left and defining the two interpolation matrices $\mathbf{B}_1 = \mathbf{U}^H$ and $\mathbf{B}_2 = \boldsymbol{\Gamma} \mathbf{V}^H$ yields

$$\begin{aligned} \mathbf{U}^H \mathbf{B} \mathbf{a}(\theta) &= \mathbf{U}^H \mathbf{U} \boldsymbol{\Gamma} \mathbf{V}^H \mathbf{a}(\theta) = \mathbf{B}_2 \mathbf{a}(\theta) \approx \\ &\approx \mathbf{U}^H \check{\mathbf{a}}(\theta) = \mathbf{U}^H \mathbf{a}(\theta) z(\theta) = \mathbf{B}_1 \mathbf{a}(\theta) z(\theta) . \end{aligned} \quad (11)$$

Clearly, the two virtual array manifolds $\check{\mathbf{a}}_1(\theta) = \mathbf{B}_1 \mathbf{a}(\theta)$ and $\check{\mathbf{a}}_2(\theta) = \mathbf{B}_2 \mathbf{a}(\theta)$ are related to each other by the shift function: $\check{\mathbf{a}}_2(\theta) \approx z(\theta) \check{\mathbf{a}}_1(\theta)$ for $\theta \in \Theta$.

It is easily verified that the sensor noise corresponding to both virtual arrays is spatially white with the noise covariance matrices

$$\check{\mathbf{Q}}_1 = \sigma_n^2 \mathbf{I} \quad \text{and} \quad \check{\mathbf{Q}}_2 = \sigma_n^2 \boldsymbol{\Gamma}^2 . \quad (12)$$

Interestingly, we observe that the noise variances of the second virtual array are proportional to the squared singular values of the interpolation matrix \mathbf{B} . In other words, there are certain virtual sensors whose signals are more degraded by sensor noise than others. It is important to note that due to the linear transformation each of the sensors of both virtual arrays generally contains information of all physical sensors.

With $\mathbf{b}_{2,i}$ representing the i th row of \mathbf{B}_2 and making use of equation (12), we define the (data independent) Signal-to-Noise Ratio (SNR) of the i th sensor in the second virtual array averaged over the representative directions as

$$\text{SNR}_i = \frac{\|\mathbf{b}_{2,i} \mathbf{C}\|^2}{K \gamma_i^2} , \quad (13)$$

where $\gamma_1, \dots, \gamma_N$ are the singular values of \mathbf{B} .

The dimension reduction of the array data in order to further reduce the computational load of the direction-finding algorithm is a primary objective of several so-called beampulse methods, for example [11]. Equation (13) provides a simple and intuitive criterion for the appropriate choice of the number of virtual sensor elements, in a sense that we simply remove those sensors of the virtual arrays which correspond to an average SNR below a given threshold τ . That is, the i th row of the interpolation matrices \mathbf{B}_1 and \mathbf{B}_2 is removed if $\text{SNR}_i < \tau$ for $i = 1, \dots, N$. This may be formulated using a suitably designed ($\bar{N} \times N$) selection matrix \mathbf{J} such that the interpolation matrices of reduced dimension are

$$\bar{\mathbf{B}}_i = \mathbf{J} \mathbf{B}_i \quad \text{for } i = 1, 2 . \quad (14)$$

4. INTERPOLATED ESPRIT

The derivation of the algorithm is very similar to the original ESPRIT approach [3]. Neglecting the interpolation errors (which means assuming the approximation (5) to be fulfilled exactly) and using equation (11), we get

$$\bar{\mathbf{B}}_1 \mathbf{A} \mathbf{Z} = \bar{\mathbf{B}}_2 \mathbf{A} \quad (15)$$

with the (unknown) physical steering matrix $\mathbf{A} = \mathbf{A}(\boldsymbol{\theta})$ and the matrix $\mathbf{Z} = \mathbf{Z}(\boldsymbol{\theta})$ containing the values of the shift function for the true DOAs $\theta_1, \dots, \theta_L$. By definition, the matrix \mathbf{E}_s from equation (3) and the steering matrix \mathbf{A} span the same subspace. Therefore, these matrices are related to each other by a full rank matrix \mathbf{T} :

$$\mathbf{A} = \mathbf{E}_s \mathbf{T} \quad (16)$$

Substituting \mathbf{A} in (15) using the last equation and multiplying with \mathbf{T}^{-1} from the right, we end up with

$$\bar{\mathbf{B}}_1 \mathbf{E}_s \Psi = \bar{\mathbf{B}}_2 \mathbf{E}_s , \quad (17)$$

where we used the definition

$$\Psi = \mathbf{T} \mathbf{Z} \mathbf{T}^{-1} . \quad (18)$$

Note that Ψ is generated from \mathbf{Z} by a similarity transformation, which means that the eigenvalues of Ψ are the diagonal elements of \mathbf{Z} . Hence, with an estimate $\hat{\Psi}$ of Ψ we can obtain estimates for the DOAs by applying the inversion formula $\hat{\theta}_l = z^{-1}(\hat{\lambda}_l)$ to the eigenvalues $\hat{\lambda}_1, \dots, \hat{\lambda}_L$ of $\hat{\Psi}$.

An estimate for the matrix Ψ can be found by solving equation (17) in a weighted least-squares sense (or similarly, in a weighted total-least-squares sense):

$$\begin{aligned} \hat{\Psi} &= \arg \min_{\Psi} \left\{ \left\| \bar{\mathbf{W}}^{\frac{1}{2}} (\bar{\mathbf{B}}_1 \hat{\mathbf{E}}_s \Psi - \bar{\mathbf{B}}_2 \hat{\mathbf{E}}_s) \right\|_F^2 \right\} \\ &= (\bar{\mathbf{W}}^{\frac{1}{2}} \bar{\mathbf{B}}_1 \hat{\mathbf{E}}_s)^\dagger \bar{\mathbf{W}}^{\frac{1}{2}} \bar{\mathbf{B}}_2 \hat{\mathbf{E}}_s \end{aligned} \quad (19)$$

The diagonal matrix $\bar{\mathbf{W}} = \mathbf{J} \mathbf{W} \mathbf{J}^T$ consists of the sensor-specific SNR values defined in equation (13) (that is, the ($N \times N$) matrix \mathbf{W} consists of all SNR values). The weighting emphasizes the influence of the virtual sensors with the highest averaged SNR. Like the interpolation matrices, the weighting matrix is independent of the sensor data and can be computed in advance.

5. SIMULATION RESULTS

In order to illustrate the various advantages of the new interpolation approach we compute the Root-Mean-Square Error (RMSE) of the DOA estimation obtained by Interpolated ESPRIT, averaged over a set of different array configuration and source signal scenarios. We consider a planar sensor array composed of $N = 15$ sensors. In each simulation run,

sensor positions are randomly drawn from a circular uniform distribution with radius $r = \lambda$ located in the x - y -plane and centered around the origin of a spherical coordinate system. Similarly, in each simulation run the locations of two uncorrelated and equipowered signal sources with a constant angular separation of $\theta_1 - \theta_2 = 8^\circ$ are drawn uniformly from the interval $[-45^\circ, 45^\circ]$. The number of snapshots is $M = 100$. In total, 1000 independent simulation runs are performed to estimate the RMSE's which are displayed in Fig. 1 versus spectral MUSIC and the corresponding averaged Cramer-Rao Bound (CRB) of the physical sensor arrays. The interpolation sector for the design of the interpolation matrices is $[-45^\circ, 45^\circ]$ (to get a fair comparison, this is also where the MUSIC spectrum was searched for peaks). The shift function is $z(\theta) = e^{j2\pi \sin(\theta)}$ and $\tau = 1/4$ is chosen as a threshold for the selection of the virtual sensors leading to an averaged virtual array length of $\bar{N} \approx 10$ sensors.

Note that averaging over the various sensor array and source location scenarios emphasizes the worst case performance of the proposed methods. Also note that conventional data independent interpolation methods like Friedlander's interpolation approach [7] completely fail to resolve the sources in the described scenarios and therefore are not helpful to be used as a benchmark.

The simulation results validate the essential performance improvement provided by the proposed method. The RMSE of the new approach is not longer limited by the bias of the DOA estimates. Its absolute value slightly exceeds the results we obtained with conventional MUSIC, but this is a small price for the huge saving in computational load and algorithm complexity. In regions of low SNR (below 15 dB in Fig. 1) Interpolated ESPRIT even outperforms spectral MUSIC, because the new algorithm shows a very favorable threshold behavior.

Furthermore, the general setting chosen in the simulations shows both the reliability of the method and the simplicity of the interpolation design which makes the method applicable to a wide class of scenarios.

6. REFERENCES

- [1] A. J. Barabell, "Improving the resolution performance of eigenstructure-based direction-finding algorithms," *Proc. ICASSP'83*, Boston, Massachusetts, pp. 336-339, May 1983.
- [2] P. Stoica and K. C. Sharman, "Maximum likelihood methods for direction-of-arrival estimation," *IEEE Trans. Acoust., Speech, Signal Processing*, vol. 38, pp. 1132-1143, July 1990.
- [3] A. L. Swindlehurst, B. Ottersten, R. Roy and T. Kailath, "Multiple invariance ESPRIT," *IEEE Trans. Signal Processing*, vol. 40, pp. 867-881, Apr. 1992.
- [4] C. P. Mathews and M. D. Zoltowski, "Eigenstructure techniques for 2-D angle estimation with uniform circular arrays," *IEEE Trans. Signal Processing*, vol. 42, pp. 2395-2407, Sept. 1994.
- [5] A. L. Swindlehurst, P. Stoica and M. Jansson, "Application of MUSIC to arrays with multiple invariances," *Proc. ICASSP'00*, Istanbul, Turkey, pp. 3057-3060, June 2000.
- [6] M. Pesavento, A. B. Gershman and K. M. Wong, "Direction of arrival estimation in partly calibrated time-varying sensor arrays," *Proc. ICASSP'01*, Salt Lake City, Utah, May 2001.
- [7] B. Friedlander, "The root-MUSIC algorithm for direction finding with interpolated arrays," *Signal Processing*, vol. 30, pp. 15-29, 1993.
- [8] J. Eriksson and M. Viberg, "Data reduction in spatially colored noise using a virtual uniform linear array," *Proc. ICASSP'00*, Istanbul, Turkey, pp. 3073-3076, June 2000.
- [9] P. Hyberg, M. Jansson and B. Ottersten, "Array mapping: optimal transformation matrix design," *Proc. ICASSP'02*, Orlando, FL, pp. 2905 -2908, May 2002.
- [10] B. Friedlander and A. J. Weiss, "Direction Finding Using Spatial Smoothing With Interpolated Arrays," *IEEE Trans. Aerospace and Electronic Systems*, vol. 28, no. 2, pp. 574-587, April 1992.
- [11] M. D. Zoltowski, G. M. Kautz and S. D. Silverstein, "Beamspace Root-MUSIC," *IEEE Trans. Signal Processing*, vol. 41, no. 1, pp. 344-364, Jan. 1993.

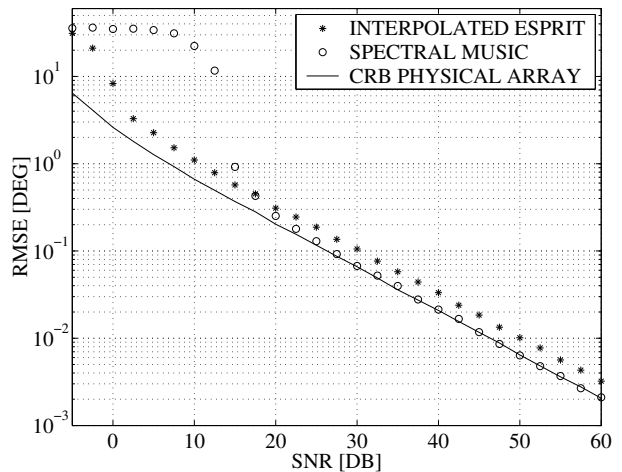


Fig. 1. RMSE of DOA estimation versus SNR.